Emerald Insight

Rapid Prototyping Journal

Improved surface finish in 3D printing using bimodal powder distribution
Michele Lanzetta Emanuel Sachs

Article information:

To cite this document:
Michele Lanzetta Emanuel Sachs, (2003),"Improved surface finish in 3D printing using bimodal powder distribution", Rapid Prototyping Journal, Vol. 9 Iss 3 pp. 157 - 166
Permanent link to this document:
http://dx.doi.org/10.1108/13552540310477463

Downloaded on: 09 November 2015, At: 07:51 (PT)
References: this document contains references to 17 other documents.
To copy this document: permissions@emeraldinsight.com
The fulltext of this document has been downloaded 1573 times since 2006*

Users who downloaded this article also downloaded:

Elena Bassoli, Andrea Gatto, Luca Iuliano, Maria Grazia Violante, (2007),"3D printing technique applied to rapid casting", Rapid Prototyping Journal, Vol. 13 Iss 3 pp. 148-155 http://dx.doi.org/10.1108/13552540710750898

David Bak, (2003),"Rapid prototyping or rapid production? 3D printing processes move industry towards the latter", Assembly Automation, Vol. 23 Iss 4 pp. 340-345 http://dx.doi.org/10.1108/01445150310501190

Robert Bogue, (2013),"3D printing: the dawn of a new era in manufacturing?", Assembly Automation, Vol. 33 Iss 4 pp. 307-311 http://dx.doi.org/10.1108/AA-06-2013-055

Access to this document was granted through an Emerald subscription provided by emerald-srm:273154 []

For Authors

If you would like to write for this, or any other Emerald publication, then please use our Emerald for Authors service information about how to choose which publication to write for and submission guidelines are available for all. Please visit www.emeraldinsight.com/authors for more information.

About Emerald www.emeraldinsight.com

Emerald is a global publisher linking research and practice to the benefit of society. The company manages a portfolio of more than 290 journals and over 2,350 books and book series volumes, as well as providing an extensive range of online products and additional customer resources and services.

Emerald is both COUNTER 4 and TRANSFER compliant. The organization is a partner of the Committee on Publication Ethics (COPE) and also works with Portico and the LOCKSS initiative for digital archive preservation.

*Related content and download information correct at time of download.

Downloaded by McGill University At 07:51 09 November 2015 (PT)

Improved surface finish in 3D printing using bimodal powder distribution

Michele Lanzetta and Emanuel Sachs

The authors

Michele Lanzetta is an Assistant Professor at the Department of Mechanical, Nuclear and Production Engineering, University of Pisa, Pisa, Italy.
Emanuel Sachs is a Professor of Mechanical Engineering, Three Dimensional Printing Laboratory, Laboratory for Manufacturing and Productivity, Massachusetts Institute of Technology, Cambridge, MA, USA.

Keywords

Rapid prototyping, Layered manufacturing, Deposition, Printing

Abstract

The use of bimodal powders has been shown to offer the possibility of dramatically improved surface finish in 3D printing. This work focused on individual lines, the primitive building block of 3D printed parts. It was observed that the fine component of bimodal ceramic powders, while uniformly distributed in the original powderbed, was preferentially found at the surface of the printed line, while the interior of the line was denuded of fines. Microscopic examination and approximate quantitative analysis supports the assertion that essentially all the fines have moved to the surface of the line. The mechanism for this rearrangement is not known, but is speculated to be related to the relative difficulty of wetting fine powders. The parameter space in which this phenomenon can be observed was examined in a preliminary manner.

Electronic access

The Emerald Research Register for this journal is available at
http://www.emeraldinsight.com/researchregister

The current issue and full text archive of this journal is available at
http://www.emeraldinsight.com/1355-2546.htm

Rapid Prototyping Journal
Volume 9 · Number 3 · 2003 · pp. 157–166
© MCB UP Limited · ISSN 1355-2546
DOI 10.1108/13552540310477463

1. Introduction

Three-dimensional printing (Sachs *et al.*, 1992, 1993) is an example of solid freeform fabrication (SFF) or layered manufacturing technology. Powdered materials are deposited in layers and selectively joined with binder from an ink-jet printhead. More recently (Sachs *et al.*, 2000), the evolution from *prototyping* to *production* is stressed for the inherent advantages of the layered method. Surface finish in 3D printing is, however, one of the major technological constraints on its widespread utilization.

Surface finish is an intrinsic limitation of powder-based processing (Ippolito *et al.*, 1995) and has been approached by authors in different ways, including the selection of the optimal build orientation (Campbell *et al.*, 2002; Xu *et al.*, 1999). The impact of the surface finish of ceramic shell moulds on cast parts has been dealt with by Jia *et al.* (2001); it is also related to the powder density, which can also be predicted as in German (1992) and Zheng *et al.* (1995).

Surface finish in 3D printed parts can be greatly improved by using very fine powders as they allow the use of thinner layers and also provide improved finish within each layer; Plate 1 shows examples of parts made with 1 μm alumina powders. But these powders have to be processed by the slurry method (Moon *et al.*, 2000) because the fine powders cannot be spread dry. In this process, powders 2 μm or less are deposited as a wet slurry. After drying the layer, binder is printed to define the component. This wet process is more complex and slower than the dry process. In addition, larger powders have preferred physical and thermal properties for some applications.

The goal of this work is to achieve dramatically improved surface finish in using dry powders in 3D printing. The specific application under consideration is the

The authors would like to thank Jim Serdy, from the 3D Printing Lab at the MIT for his invaluable help and advice from his immeasurable experience. Professor Michael Cima and the other members of the "ceramics group" are acknowledged for their useful suggestions.

The Italian National Research Council (CNR), under the Short Term Mobility Program, is gratefully acknowledged for its financial support.
Received: 7 December 2001
Reviewed: 5 August 2002
Accepted: 28 February 2003

Downloaded by McGill University At 07:51 09 November 2015 (PT)

Plate 1 Functional parts 3D printed with the "slurry" method and detail of the surface

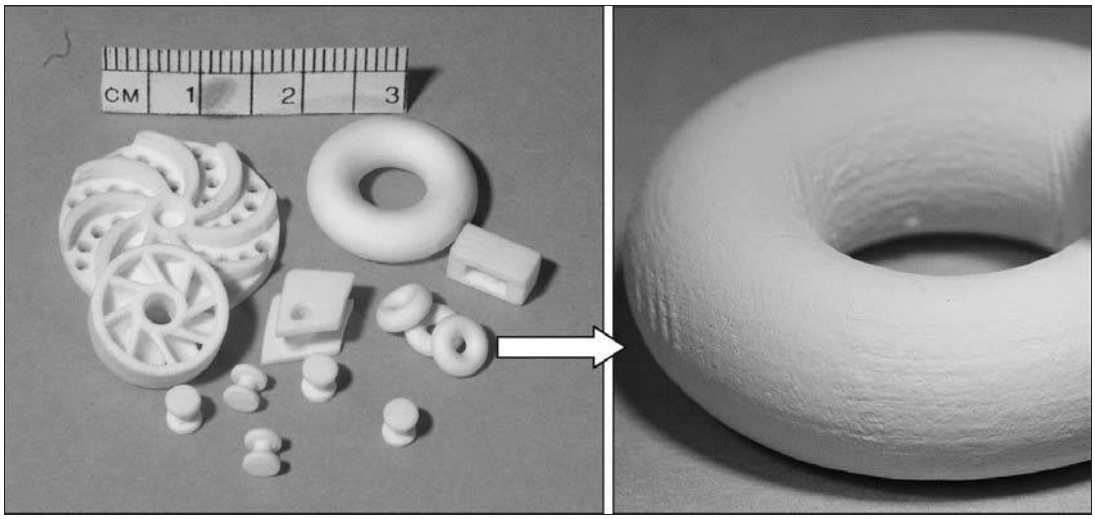

fabrication of ceramic molds for metal casting using alumina powders (rapid tooling). However, improved surface finish with dry powder processing will be of widespread application in 3D printing technology.

1.1 Current work

This work examines the surface finish of individual line segments. As 3D printed parts are made by the assembly of many such individual line segments, it is felt that this is the simplest case that can be meaningfully examined (Lanzetta and Sachs, 2001a, b).

A line printed with a 20 μm spherical alumina powder (Alunabeads CB-A20S) shows the quality attained with a unimodal powder (Plate 2).

The beneficial effects of bimodal distributions of powders are well known (German, 1992, 1994) and are exploited in applications such as powder injection molding, slip casting and sintering. The main properties of bimodal powders include:

- improving the surface finish, by having the small grains fill the voids among the large grains;
- increasing the packing density for the above reason, according to the size ratio of the two main components.

In this work, experiments have been carried out to assess the behaviour of different bimodal distributions in 3D printing with dry powders.

Regarding the printing technology (Heinzl and Hertz, 1985), a drop-on-demand (DoD) printhead has been selected because it yields smaller drops, allowing a higher process resolution than the continuous jet. Another advantage of the DoD technology is the better performance in vector printing, which is also indicated in applications where the quality requirements are critical (Sachs *et al.*, 2000). In vector printing, the execution of curved trajectories and the associated speed changes require controlling the drop frequency in a wide range, which is only possible with DoD.

2. Experimental technique

2.1 Printhead and machine

An HP DoD ink-jet cartridge model 51626A (HP, 1999) was used for this work. This

Plate 2 SEM image of the line surface with a 20 μm spherical alumina powder

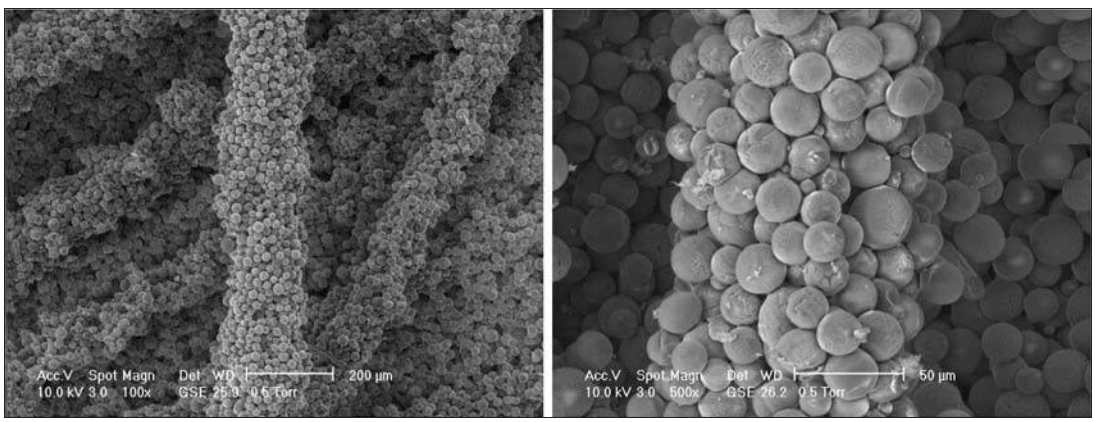

Downloaded by McGill University At 07:51 09 November 2015 (PT)

Rapid Prototyping Journal
Volume 9 · Number 3 · 2003 · 157–166

printhead is based on the thermal or evaporative bubble principle (Heinzl and Hertz, 1985). With the unusual material used for this work (see later), the printhead could be operated at speeds of up to 1.5 kHz to produce droplets which range in a diameter from 50 to 70 μm at speeds of 15 ± 1.5 m/s. This printhead was positioned between 1 and 8 mm from the powderbed (little effect of different printhead distances was noted).

The lines observed have been printed (Figure 1) using a semi-automatic machine (Lanzetta and Sachs, 2001c), which has been developed in order to explore the more suitable range of the main process parameters. The powderbed is moved at the selected speed on a linear ball-bearing guide to insure a regular movement in the whole speed range. Parallel lines are printed on the same bed by moving the printhead between passes on a secondary controlled axis. An electronic circuit generates the necessary signal profile to drive the printhead (at the selected voltage). Only one nozzle at a time is used. The drop frequency and the line spacing are controlled via PC.

2.2 The material system

The bimodal powders consist of a large powder (referred to as the "main powder") and a smaller "additive".

The main powders tested include single size 20 and 30 μm spherical alumina made by plasma spherodization (Alunabeads CB-A20S and CB-A30S). Spherical powders have been found to produce the best surface finish for unimodal distributions, presumably owing to their ability to pack together well. Finer powders have the potential for improved surface finish; however, cohesive forces between the powders make them more difficult to spread. Thus, it was found that 10 μm spherical powder was significantly harder to spread than the 20 μm powder primarily used in this study (Plate 3, top).

Two smaller additive powders were used in this work: a 2.5 μm platelet shaped powder (Electro-abrasives F1200) and a 5 μm equiaxial alumina powder (Suritomo chemical). In the mixtures tested, between 10 and 25 per cent by weight of additive powder has been used. The mixing has been done by shaking the two powders in a small bottle for about 10 min, continuously changing the direction and the speed of movement to avoid segregation. After shaking, the powder was sieved, with a 325 (44 μm) sieve, to improve

Figure 1 Configuration of the line-printing machine

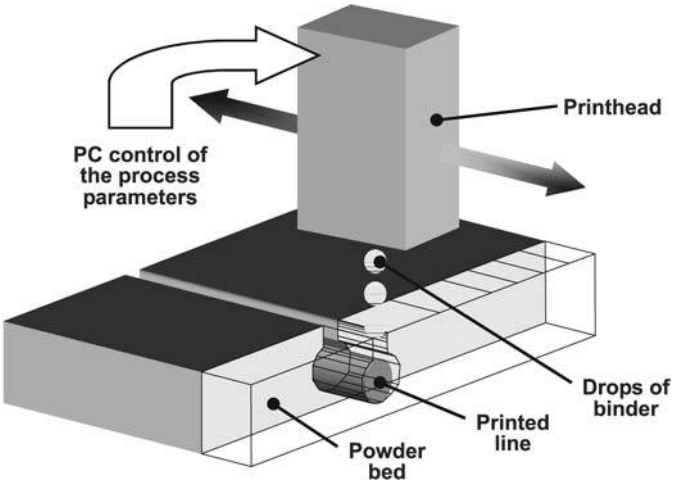

Plate 3 SEM images. Details of the main powder (20 μm spherical alumina) and two additives: 2.5 μm platelet (center) and 5 μm equiaxial (bottom)

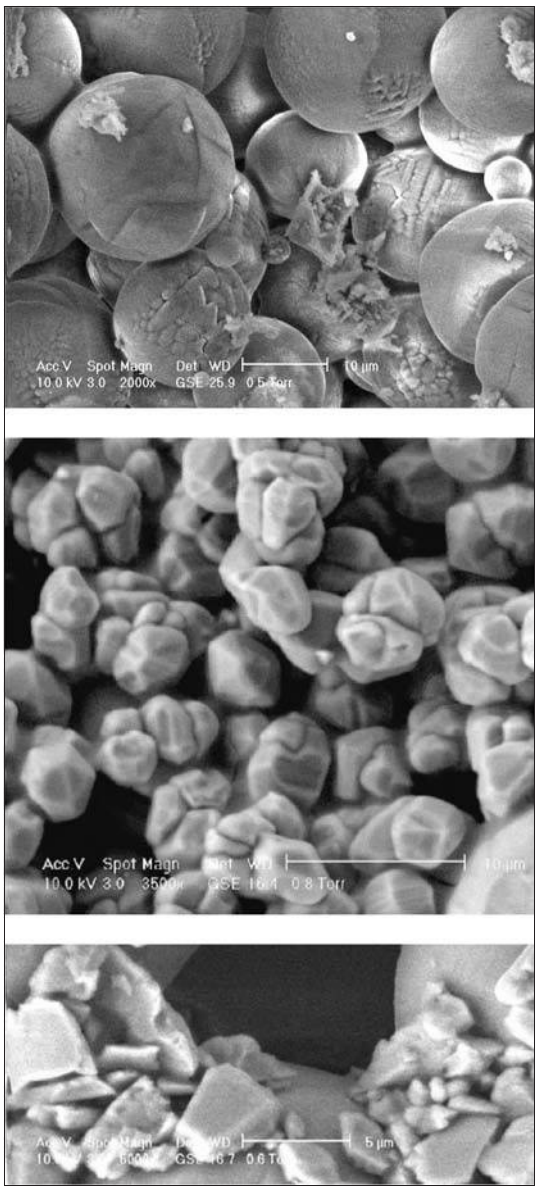

Downloaded by McGill University At 07:51 09 November 2015 (PT)

Rapid Prototyping Journal
Volume 9 · Number 3 · 2003 · 157–166

mixing and to remove clumps that are likely to occur with small powders, for their tendency to absorb humidity.

The binder used was a silica solution in ethylene glycol which is provided at 20.8 per cent wt silica content (Nissan Chemical Industries EG-ST). This material was diluted with water in the ratio of 1:1. The use of ethylene glycol based colloidal silica avoided the problem of nozzle clogging by drying which was encountered with aqueous colloidal silica, although aqueous materials are the standard in investment casting practice.

2.3 The process parameters

The three process parameters related to droplet deposition are:

- printhead speed – the speed of traverse of the printhead over the powderbed;
- drop frequency – the frequency of droplet deposition;
- droplet spacing – the spacing between droplets.

These parameters are related as follows:

$$\text{Printhead speed} = \text{Drop spacing} \times \text{Drop frequency}$$

The parameter space was narrowed by fixing the printhead speed at a convenient value of 8 mm/s. This speed is fast enough to allow for economical production of important classes of small, fine-featured parts, yet slow enough to allow for extremely accurate path fidelity during vector traversing. For a given formulation of powderbed, a range of drop spacing and drop frequency were explored with the intent of finding parameters which resulted in good surface finish. For the exemplar lines shown in the figures, the drop spacing is stated in the caption and the drop frequency may be calculated, given a printhead speed of 8 mm/s.

3. Observations and discussion

3.1 The formation of lines

The interaction of liquid droplets with the powderbed involves the dissipation of the kinetic energy of the droplets, engulfing powder particles into the droplets, infiltration of the liquid into the powderbed, and rearrangement of the powder under capillary forces. Plate 4 shows the formation of small, roughly spherical aggregates of particles due to the interaction of single drops from a DoD printhead with the powderbed. The spherical shape is the result of the capillary rearrangement of the powder so as to minimize surface energy.

When droplets are printed close together they overlap, a cylindrical line generally results, due to the minimization of surface energy by capillary forces. (In such circumstances, generally with powder that is not well wetted by the liquid binder, the capillary forces actually result in the formation of a series of large, disconnected balls, a condition of even lower surface area than that of the continuous line. However, the powders used in this study are ceramic and are well wetted.) Plate 5 shows the formation of a line in 30 μm platelet shaped alumina powder under the action of droplets from a continuous-jet printhead (Straube, 2000). These droplets are 90 μm in diameter and travel at a speed of 10 m/s, and arrive a frequency of 40 kHz. The combination of large drops arriving at high frequency results in considerable ejection of powder and the formation of a trench. The roughly cylindrical line may be seen lying at the bottom of the trench, retracted inward from the walls of the trench.

However, in the present work, using DoD printheads result in significantly lower droplet frequencies and smaller droplet size, the cylindrical lines have been observed to form partly submerged in the powder as shown in Plates 6 and 7. Observation shows a groove, corresponding in width roughly the diameter of the droplets, with a larger cylindrical line buried under the powder. Plate 7 shows a particularly large diameter line printed with small drop spacing.

3.2 Bimodal powderbeds

The focus of this study is on bimodal powders. Qualitatively, comparing the unimodal line displayed in Plate 2 with the bimodal lines in Plates 8 and 9, the lines made with bimodal powders are more regular and have a better surface finish. From a closer view, such as that of Plate 10, it can be observed that the improved surface finish is due to a smoothing effect where the small additive powder fills the gaps between the larger main powder. In Plate 10, the additive powder is 5 μm equiaxial. In Plate 11, a similar effect can be seen in a case where the additive powder is 2.5 μm and platelet in shape. In both cases,

Downloaded by McGill University At 07:51 09 November 2015 (PT)

Plate 4 SEM images. Top view of single-drop primitives in a powderbed. The ejection and contraction are clearly visible

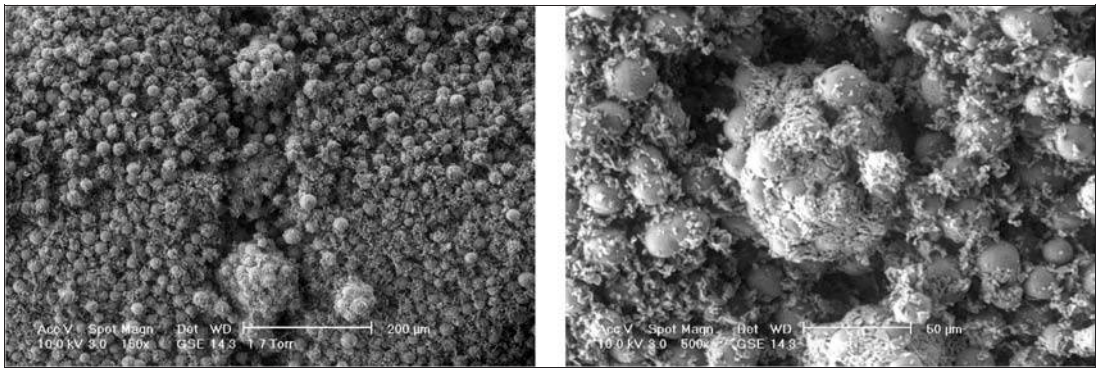

Plate 5 High-speed frame (top) of the drop impact and the line formation in continuous jet printing with large equiaxial alumina powder. The powder ejection is clearly visible and it does not depend on the grain shape. Detail of a line (bottom) lying in the wide groove formed within the bed

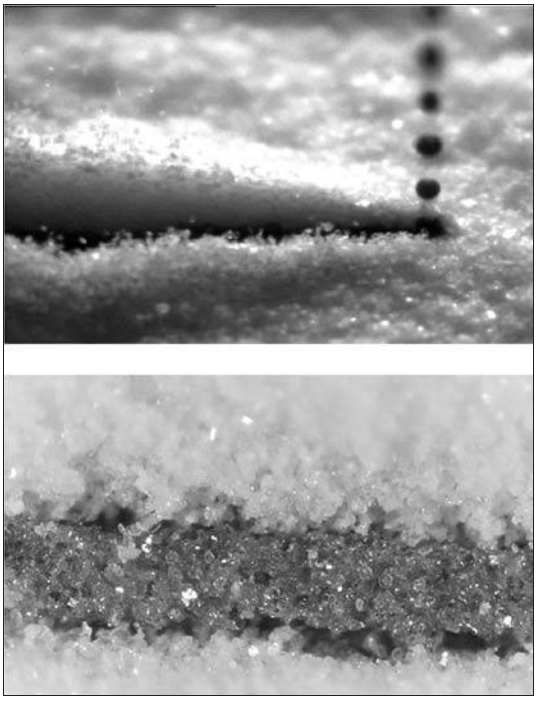

some of the voids have not been filled by the additive powder.

Comparing the line surface of Plates 9 and 11 with a top view of the original powderbed (Plate 6, detail) a higher concentration of small particles is observed on the line surface. The cross-sections of lines shown in Plates 12 and 13 make it clear that, while the exterior of the lines has a heavy concentration of fine particles, the interior is denuded of fines. These observations suggest that during the formation of the line, the fines within the powder which will form the line becomes concentrated on the exterior of the line.

While not an exhaustive study, the results do indicate a similar behaviour over a range of fine powder size (2.5 and 5 μm), shape (equiaxial and platelet) and concentration (12.5 and 25 per cent wt). Note that, not surprisingly, the case of 25 per cent wt gives a more complete coating. Further, it is likely that concentrations higher than 25 per cent wt would create significant difficulties in spreading the powders due to the increased agglomeration of the powder.

Plate 6 SEM images. Top view (left) of a line submerged in a powderbed and groove made by the binder drops. 20 μm spherical with 25 per cent wt 2.5 μm platelet alumina powder. Detail of the same powderbed (right)

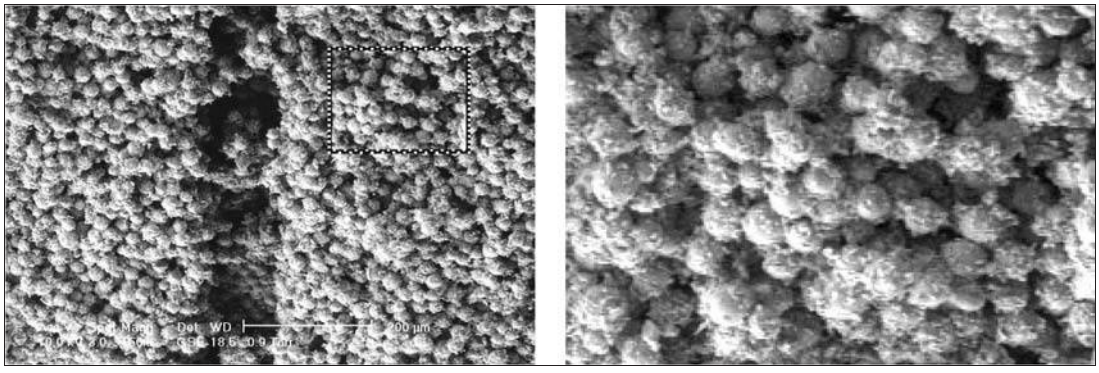

Downloaded by McGill University At 07:51 09 November 2015 (PT)

Rapid Prototyping Journal
Volume 9 · Number 3 · 2003 · 157–166

Plate 7 SEM image. A partially (bottom) uncovered large line made with 20 μm spherical with 25 per cent wt 2.5 μm platelet alumina powder; drop spacing: 5 μm

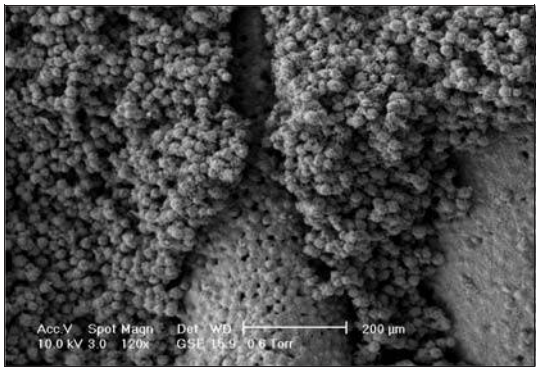

Plate 8 SEM image of a good line made with 20 μm spherical with 12.5 per cent wt 5 μm equiaxial alumina powder; drop spacing: 10 μm

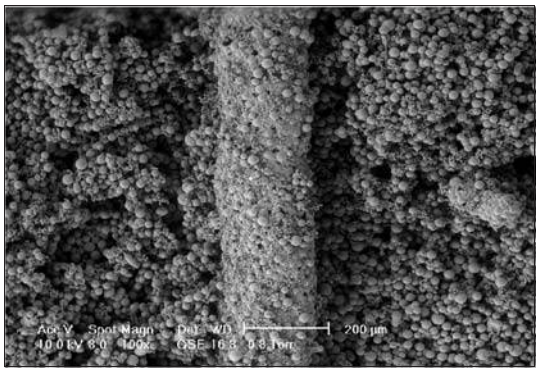

Plate 9 SEM image of good lines made with 20 μm spherical with 25 per cent wt 2.5 μm platelet alumina powder; drop spacing: 7 μm

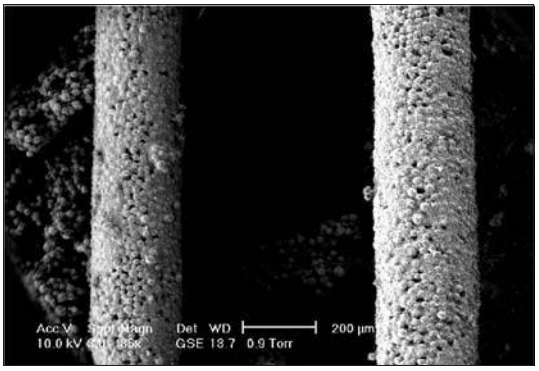

3.2.1 Estimating the rearrangement

The hypothesis that the fines from the powder of the interior of the line have moved to the exterior can be examined by calculating the coating thickness that would result from such rearrangement. Let V_R represent the ratio of the volume of the small and the large grains. Suppose that all the fines have redistributed to the exterior in an uniform coating of thickness C_t, around a cylindrical line of radius L_R. The volume ratio can be calculated as:

$$V_R = \frac{2\pi L_R C_t}{\pi L_R^2} = 2\frac{C_t}{L_R} \quad (1)$$

In this case, both the main powder and the fine additive are alumina and so, the volume ratio is the same as the weight ratio. In the application to the case of Plates 8, 10 and 12, where 5 μm particles are used, it can be assumed that the coating thickness is a single layer of particles as evident in Plate 12. Assuming a line radius of 65 μm as in Plate 12, a volume ratio of 14 per cent is calculated – very close to the mixed ratio of 12.5 per cent. This further supports the hypothesis that the fines have moved to the exterior of the line from the powder which makes up the line.

The above simple geometrical relation also shows that, when printing thinner lines, the same coating thickness is obtained with a lower weight ratio. In Plate 10 (top and bottom), lines of different thickness from the same bed seem to have the same concentration of small powder. This probably means that there is an upper limit to the available coating thickness.

The application of equation (1) to the cases of Plates 10 and 13 predicts that if all the fine powder has moved to the surface, then the coating should be about 10 μm (or five particles) thick. This is in keeping with the micrographs of the lines.

3.2.2 Interaction between line and bed

The printed lines are revealed by removing the unprinted powder using an air jet. During such procedures, a small gap has been observed between the printed line and the powderbed around it, as evidenced in the lower half of Plate 7.

In the fabrication of a glass bonded ceramic, the common practice in 3D printing is to fire the entire powderbed with the printed region still embedded in it. The firing sinters the glass bond and creates a stronger body while the surrounding powder supports the part during the firing and minimizes distortion. When fired at temperatures of up to 1,000°C, the bimodal lines separate cleanly from the surrounding powderbed. This is attributed to two factors: the gap between the lines and the surrounding powderbed, as noted above, and the smooth surface of the bimodal lines does not contain protruding

Downloaded by McGill University At 07:51 09 November 2015 (PT)

Plate 10 SEM images. A larger (top) and a smaller (bottom left) line made of 20 μm spherical with 12.5 per cent wt 5 μm equiaxial alumina powder. Detail of the line surface (bottom right) showing the concentration of small grains. Drop spacing: 12 μm (top), 40 μm (bottom)

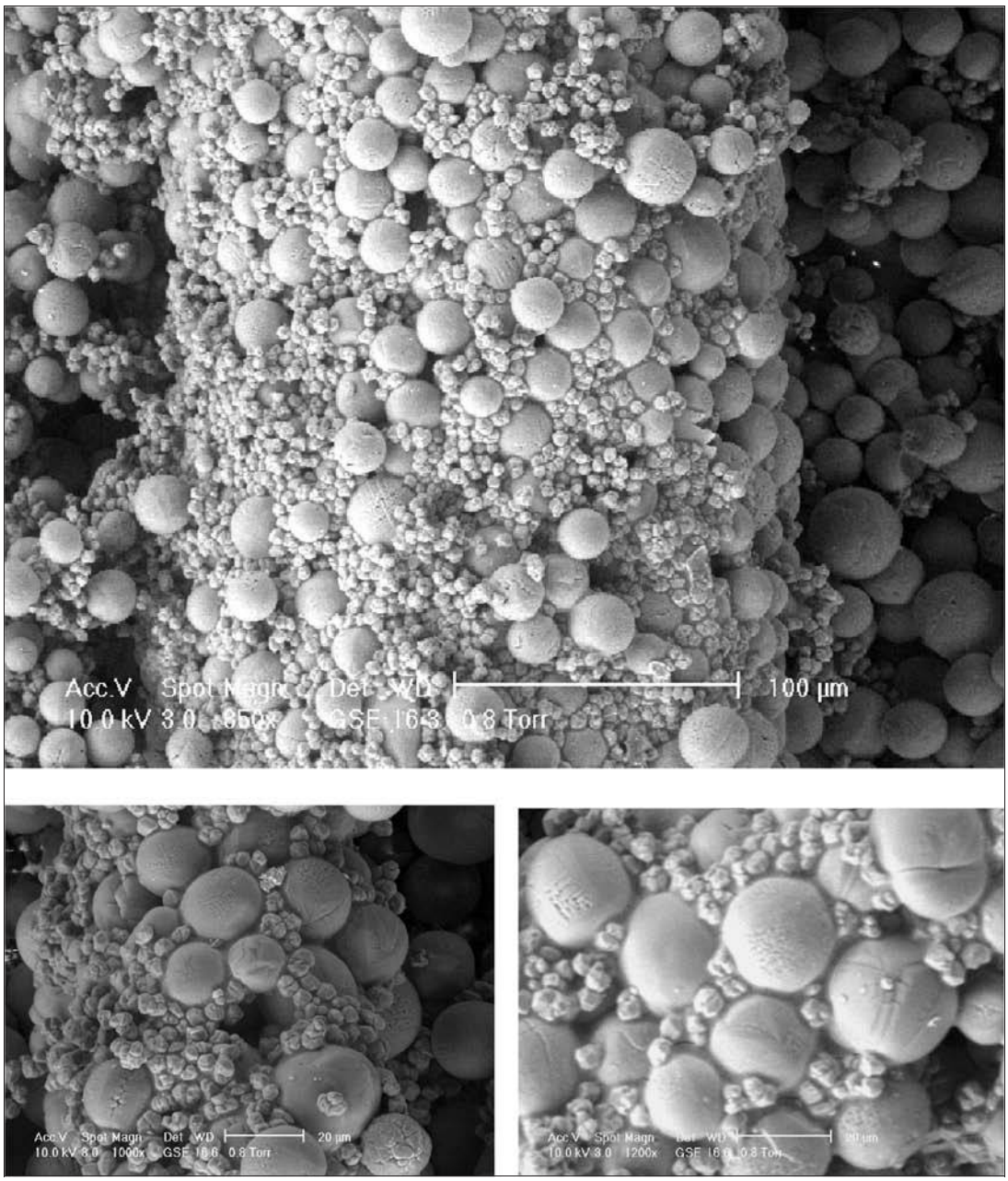

Plate 11 SEM image of a good line made with 20 μm spherical with 25 per cent wt 2.5 μm platelet alumina powder; drop spacing: 7 μm

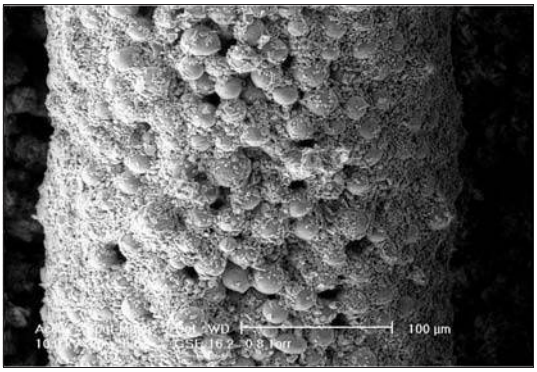

Plate 12 SEM image of a line section showing the internal part of a line made with 20 μm spherical alumina powder, partially denuded of the 12.5 per cent wt 5 μm equiaxial alumina powder additive; drop spacing: 25 μm

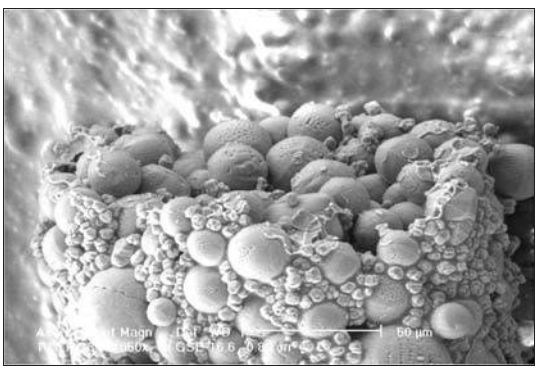

Downloaded by McGill University At 07:51 09 November 2015 (PT)

Plate 13 SEM images of line sections showing the internal part of lines made with 20 μm spherical alumina powder, partially denuded of the 25 per cent wt 2.5 μm platelet alumina powder additive; drop spacing: 7-8 μm

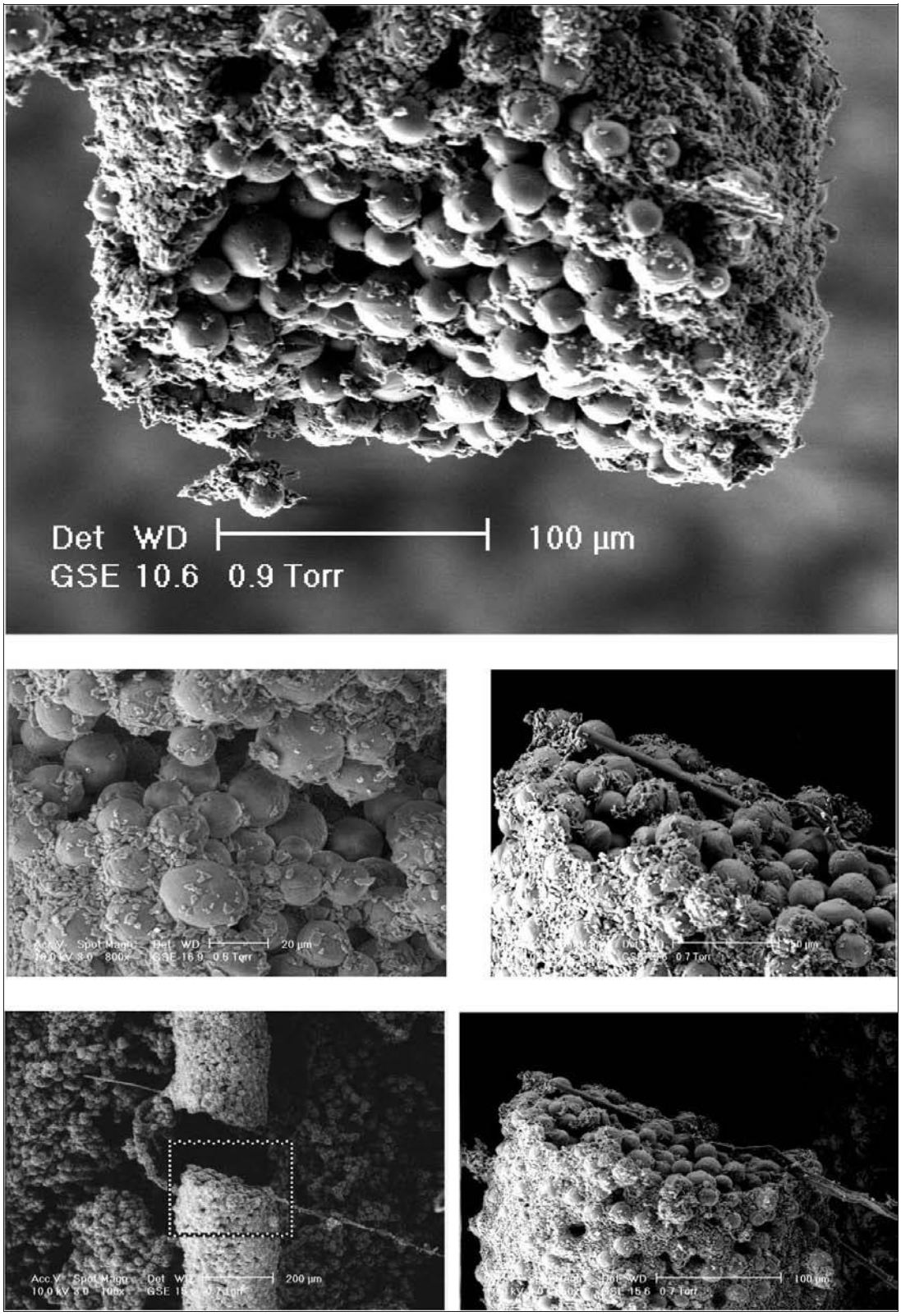

grains which would act like an anchor for the loose powder.

3.3 The effects of drop spacing

The maximum theoretical drop spacing to print a line is given by the size of the primitive single-drop. It has been observed that the smoothing noted with bimodal powders is most effective when the drop spacing is 25 μm and smaller. However, reducing the drop spacing results in a higher dosage of binder and will therefore result in lines of larger diameter, thereby degrading resolution.

Downloaded by McGill University At 07:51 09 November 2015 (PT)

Rapid Prototyping Journal
Volume 9 · Number 3 · 2003 · 157–166

The relationship between drop spacing and line diameter can be developed by assuming that the binder wicks out into the powderbed and is distributed uniformly through the cross-section of a line. Further, it is assumed that the degree of wicking depends only on the properties of the binder and powderbed and not on the dosage of binder. Under these assumptions, it can be observed that the cross-sectional area of the printed line should be proportional to the binder dose and therefore inversely proportional to the drop spacing. It follows that:

$$\text{line\_diameter} = \frac{K}{\sqrt{\text{drop\_spacing}}} \qquad (2)$$

where K is a constant that will depend on the combination of binder and powderbed.

Figure 2 shows the experimental data for 20 μm unimodal spherical powder over a range of drop spacing and the model of equation (2), where the constant K has been fitted by least squares. The agreement is quite good.

4. Conclusions

The interaction of powder and binder is the central physical interaction underlying the 3D printing process. This interaction is especially critical to the attainment of good surface finish with the technology. This work has demonstrated that bimodal powders have the potential to result in much improved surface finish, at least in the formation of individual lines – the building blocks of 3D printed parts.

The fine component of the bimodal powder was uniformly distributed in the powderbed prior to printing. However, the surprising and useful result attained was that the fines were found to be preferentially located at the surface of the line after printing. In this manner, the fines were able to provide very effective smoothing of the surface of the line. Indeed, nearly all the fines were found on the surface of the lines and little in the interior. Further, the amount of fines at the surface closely matches the hypothesis that all the fines in the powderbed that was bound by binder have migrated or moved to the surface of the lines.

The mechanism for this movement of fines to the surface of the lines is not known. One speculation is that during the interaction of binder and powder, the larger component of the powder readily enters the binder liquid, but the fines are more difficult to wet. This might lead to a coating of fines on the surface of the line during the drying process. However, elucidation of this mechanism and its extension to whole layers and then multiple layers will await further effort.

Some sense of a range of parameters over which this "coating" effect can be created was attained experimentally, including the demonstration of the effect with two different powders as fines. These powders differed in both size and shape. Further ranges of droplet spacing were explored and the effect of droplet spacing on line diameter was verified to follow a simple model based on a constant, but material specific, saturation of the powderbed with binder.

Figure 2 The line diameter as a function of the drop spacing for a 20 μm spherical alumina powder

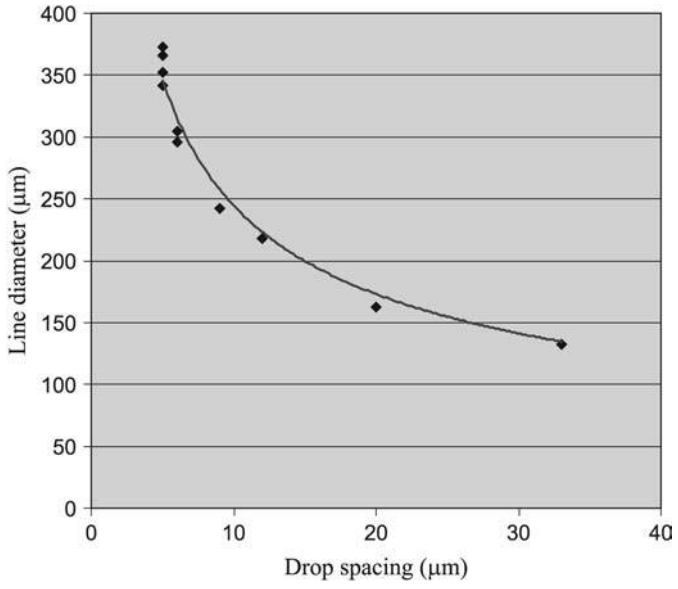

References

Campbell, R.I., Martorelli, M. and Lee, H.S. (2002), "Surface roughness visualisation for rapid prototyping models", *CAD-Computer Aided Design*, Vol. 34 No. 10, pp. 717-25.

German, R.M. (1992), "Prediction of sintered density for bimodal powder mixtures", *Metallurgical Transactions A (Physical Metallurgy and Materials Science)*, Vol. 23A No. 5, ISSN: 0360-2133, pp. 1445-65.

German, R.M. (1994), "Powder metallurgy science", *Metal Powders Industries Federation*, 2nd ed.

Heinzl, J. and Hertz, C.H. (1985), "Ink-jet printing", *Advances in Electronics and Electron Physics*, Academic Press, London, Vol. 65, pp. 91-171.

Hewlett Packard (1999), Product Safety Information Sheet, 51626 Series, 30 August 1999.

Downloaded by McGill University At 07:51 09 November 2015 (PT)

Ippolito, R., Juliano, L.P. and Gatto, A. (1995), "Benchmarking of rapid prototyping techniques in terms of dimensional accuracy and surface finish", *Annals of the CIRP*, Vol. 44 No. 1, pp. 157-60.

Jia, Q., Cui, Y.Y. and Yang, R. (2001), "Influence of powder-size matching on the surface quality of ceramic mould shell for investment casting of titanium alloys", *International Journal of Materials and Product Technology*, Vol. 2 (spec. iss.), ISSN: 0268-1900, pp. 793-8.

Lanzetta, M. and Sachs, E. (2001a), "Development of a semiautomatic machine for the drop on demand three dimensional printing", in Galantucci, L. (Ed.), A.I.Te.M V, *Proceedings of the 5th Conference of the Italian Association of Mechanical Technology*, 18-20 September 2001, Bari, Italy, Vol. 1, ISBN: 88-900637-0-X, pp. 129-44.

Lanzetta, M. and Sachs, E. (2001b), "Optimization of the line quality with dry powders in three dimensional printing", in Lonardo, P.M. (Ed.), *PRIME 2001, 1st International Seminar on: PRogress in Innovative Manufacturing Engineering*, 20-22 June 2001, Sestri Levante (GE), Italy, ISBN: 88-900559-0-1, pp. 197-204.

Lanzetta, M. and Sachs, E. (2001c), "The line formation with alumina powders in drop on demand three dimensional printing", in Lonardo, P.M. (Ed.), *PRIME 2001, 1st International Seminar on: PRogress in Innovative Manufacturing Engineering*, 20-22 June 2001, Sestri Levante (GE), Italy, ISBN: 88-900559-0-1, pp. 189-96.

Moon, J., Grau, J.E., Cima, M.J. and Sachs, E.M. (2000), "Slurry chemistry control to produce easily redispersible ceramic powder compacts", *Journal of the American Ceramic Society*, Vol. 83 No. 10, pp. 2401-3.

Sachs, E., Cima, M., Williams, P., Brancazio, D. and Cornie, J. (1992), "Three-dimensional printing: rapid tooling and prototypes directly from a CAD model", *Transaction of the ASME, Journal of Engineering for Industry*, Vol. 114, pp. 481-8.

Sachs, E., Haggerty, J., Cima, M. and Williams, P. (1993), *Three dimensional Printing Techniques*, US Patent # 5,204,055 04/28/1993.

Sachs, E., Hallen, S., Cima, M. and Raynerson, M. (2000), "Three dimensional printing: a candidate for the production of metal parts", *PM²TEC 2000 Conf.*, June 2000, New York City.

Straube, A.M. (2000), *Observation of Droplet Impacts and Line Formation in Alumina Powder in Three Dimensional Printing*, Diplomarbeit, NY, USA, MIT, MA, USA.

Xu, F., Loh, H.T. and Wong, Y.S. (1999), "Considerations and selection of optimal orientation for different rapid prototyping systems", *Rapid Prototyping Journal*, Vol. 5 No. 2, ISSN: 1355-2546, pp. 54-60.

Zheng, J., Carlson, W.B. and Reed, J.S. (1995), "The packing density of binary powder mixtures", *Journal of the European Ceramic Society*, Vol. 15 No. 5, pp. 479-83.

Downloaded by McGill University At 07:51 09 November 2015 (PT)

This article has been cited by:

1. Shu Cao, Yang Qiu, Xing-Fang Wei, Hong-Hai Zhang. 2015. Experimental and theoretical investigation on ultra-thin powder layering in three dimensional printing (3DP) by a novel double-smoothing mechanism. *Journal of Materials Processing Technology* **220**, 231-242. [CrossRef]
2. Seyed Farid Seyed Shirazi, Samira Gharehkhani, Mehdi Mehrali, Hooman Yarmand, Hendrik Simon Cornelis Metselaar, Nahrizul Adib Kadri, Noor Azuan Abu Osman. 2015. A review on powder-based additive manufacturing for tissue engineering: selective laser sintering and inkjet 3D printing. *Science and Technology of Advanced Materials* **16**, 033502. [CrossRef]
3. Shu Cao, Xing-Fang Wei, Zhen-Jun Sun, Hong-Hai Zhang. 2015. Investigation on urea-formaldehyde resin as an in-powder adhesive for the fabrication of Al2O3/borosilicate–glass composite parts by three dimensional printing (3DP). *Journal of Materials Processing Technology* **217**, 241-252. [CrossRef]
4. Truong Do, Chang Seop Shin, Dalton Stetsko, Grayson VanConant, Aleksandr Vartanian, Shenli Pei, Patrick Kwon. 2015. Improving Structural Integrity with Boron-based Additives for 3D Printed 420 Stainless Steel. *Procedia Manufacturing* **1**, 263-272. [CrossRef]
5. I. Pires, B. Gouveia, J. Rodrigues, R. Fonte. 2014. Characterization of sintered hydroxyapatite samples produced by 3D printing. *Rapid Prototyping Journal* **20**:5, 413-421. [Abstract] [Full Text] [PDF]
6. James D. Mcguffin-CawleyManufacturing Technology: Rapid Prototyping 415-437. [CrossRef]
7. Sebastian Spath, Hermann Seitz. 2014. Influence of grain size and grain-size distribution on workability of granules with 3D printing. *The International Journal of Advanced Manufacturing Technology* **70**, 135-144. [CrossRef]
8. Mohammad Vaezi, Hermann Seitz, Shoufeng Yang. 2013. A review on 3D micro-additive manufacturing technologies. *The International Journal of Advanced Manufacturing Technology* **67**, 1721-1754. [CrossRef]
9. A. Butscher, M. Bohner, N. Doebelin, L. Galea, O. Loeffel, R. Müller. 2013. Moisture based three-dimensional printing of calcium phosphate structures for scaffold engineering. *Acta Biomaterialia* **9**, 5369-5378. [CrossRef]
10. J. Suwanprateeb, F. Thammarakcharoen, K. Wasoontararat, W. Suvannapruk. 2012. Influence of printing parameters on the transformation efficiency of 3D-printed plaster of paris to hydroxyapatite and its properties. *Rapid Prototyping Journal* **18**:6, 490-499. [Abstract] [Full Text] [PDF]
11. James D. Mcguffin-CawleyManufacturing Technology: Rapid Prototyping 415-437. [CrossRef]
12. Andre Butscher, Marc Bohner, Christian Roth, Annika Ernstberger, Roman Heuberger, Nicola Doebelin, Philipp Rudolf von Rohr, Ralph Müller. 2012. Printability of calcium phosphate powders for three-dimensional printing of tissue engineering scaffolds. *Acta Biomaterialia* **8**, 373-385. [CrossRef]
13. M. Gurr, R. MülhauptRapid Prototyping 77-99. [CrossRef]
14. Mohammad Vaezi, Chee Kai Chua. 2011. Effects of layer thickness and binder saturation level parameters on 3D printing process. *The International Journal of Advanced Manufacturing Technology* **53**, 275-284. [CrossRef]
15. Xubao Wang, Tiechuan Zuo. 2010. Limit of accuracy in laser fabrication with metal powder. *Frontiers of Optoelectronics in China* **3**, 190-193. [CrossRef]
16. Ben R. Utela, Duane Storti, Rhonda L. Anderson, Mark Ganter. 2010. Development Process for Custom Three-Dimensional Printing (3DP) Material Systems. *Journal of Manufacturing Science and Engineering* **132**, 011008. [CrossRef]
17. Fabienne C. Fierz, Felix Beckmann, Marius Huser, Stephan H. Irsen, Barbara Leukers, Frank Witte, Özer Degistirici, Adrian Andronache, Michael Thie, Bert Müller. 2008. The morphology of anisotropic 3D-printed hydroxyapatite scaffolds. *Biomaterials* **29**, 3799-3806. [CrossRef]
18. Ben Utela, Duane Storti, Rhonda Anderson, Mark Ganter. 2008. A review of process development steps for new material systems in three dimensional printing (3DP). *Journal of Manufacturing Processes* **10**, 96-104. [CrossRef]
19. Aditad Vasinonta, Jack L. Beuth, Michelle Griffith. 2007. Process Maps for Predicting Residual Stress and Melt Pool Size in the Laser-Based Fabrication of Thin-Walled Structures. *Journal of Manufacturing Science and Engineering* **129**, 101. [CrossRef]
20. St. H. Irsen, B. Leukers, Chr. Höckling, C. Tille, H. Seitz. 2006. Bioceramic Granulates for use in 3D Printing: Process Engineering Aspects. *Materialwissenschaft und Werkstofftechnik* **37**:10.1002/mawe.v37:6, 533-537. [CrossRef]
21. D. Z. Wang, S. N. Jayasinghe, M. J. Edirisinghe. 2005. Instrument for electrohydrodynamic print-patterning three-dimensional complex structures. *Review of Scientific Instruments* **76**, 075105. [CrossRef]
22. J. Kim, T.S. Creasy. 2004. Selective laser sintering characteristics of nylon 6/clay-reinforced nanocomposite. *Polymer Testing* **23**, 629-636. [CrossRef]

Downloaded by McGill University At 07:51 09 November 2015 (PT)